Available online at www.sciencedirect.com

ScienceDirect

Procedia Engineering 66 (2013) 608 – 614

Procedia Engineering

www.elsevier.com/locate/procedia

5th Fatigue Design Conference, Fatigue Design 2013

Fatigue damage assessment of alternator fans by EBSD

J.-B. Vogt[a], J. Bouquerel[a], F. Léaux[a] and F. Palleschi[b]

[a]*UMET – UMR CNRS 8207, team Métallurgie Physique et Génie des Matériaux. Université Lille1, 59655 Villeneuve d'Ascq, France*
[b] *VALEO Systèmes Electriques, 2, rue André Boulle, 94046 Créteil*

Abstract

Components of new car alternators are subjected fatigue damage due to the start-stop cycles. Predicting their fatigue life still requires needs an experimental validation. Hence, identification of both monotonic and cyclic behaviour is required to integrate the right values in the models. Therefore a precise analysis of the dislocation arrangement produced by cyclic plasticty appears as a fatigue damage indicator. Here SEM-EBSD provide two plasticity markers: the Kernel Average Misorientation and the Low Angel Grain Boundaries that characterize dislocations arrangements in a quantitative way.
Based on these indexes, the comparison between lab fatigue specimens and component gives an estimation of the local cyclic plastic strain.

Keywords: Fatigue, EBSD based damage criteria, TEM, local deformation estimation

1. Introduction

The shape of alternator cooling fans may exhibit very special design according to the functions they are supposed to provide. For new machines with the stop start function to be incorporated in cars, the shape of the fan is very complex (Fig. 1) since it must evacuate heat, be light and silent.

The presence of slots at the blade root can act as stress concentrator. Thus, even if the major part of the fan is elastically loaded, yielding can occur in the vicinity of some slots as pointed out by Finite Element Method (FEM) calculations (see Fig. 1). Moreover, the operating mode of a start and stop alternator leads to cumulated localized plastic straining and then, Low Cycle Fatigue (LCF) failure can occur.

doi:10.1016/j.proeng.2013.12.112

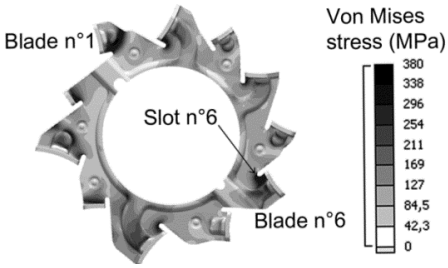

Fig. 1. Shape of the fan

The aim of the current study is to document the LCF behaviour of a ferritic steel generally employed for a fan blade. For their integrity, LCF resistance must be assessed for fatigue design and fatigue mechanisms must be understood in order to establish fatigue damage indicators. A previous experience [1] has been successfully applied on ferrite-bainitic steels by using deep TEM analysis of dislocations cells. Fatigue damage could be determined but the method only based on TEM diffraction remained tough. The methodology described in the present paper consists at first in an identification of the LCF behaviour (stress response to strain cycling, Manson Coffin relation) from experiments conducted on lab specimen. Then the evolution of the microstructure is studied through TEM investigation of dislocation structures and through SEM-EBSD analysis of the fractured specimen. Finally, SEM-EBSD analysis is carried out on a damaged fan and allows determination of fatigue loading.

2. Experimental procedure

2.1. Material

The chemical composition of the steel is given in Table 1. The low carbon steel had a ferritic equiaxed microstructure and a grain size of 11µm.

Table 1. Chemical composition (wt.%) of the studied ferritic steel (according to JIS G3141 norm)

Fe	C	Si	Mn	P	S
Bal.	0.0346	0.002	0.228	0.0063	0.0041

The conventional monotonic mechanical properties are reported in Table 2

Table 2. Chemical composition (wt.%) of the studied ferritic steel (according to JIS G3141 norm)

Fe	C	Si	Mn	P	S
Bal.	0.0346	0.002	0.228	0.0063	0.0041

2.2. Fatigue testing

The fatigue specimens were plate with a thickness of 1.2mm, a width of 8mm and a gauge length of 15mm. The LCF fatigue tests were performed at room temperature with a triangular wave form, using a MTS hydraulic machine with a load capacity of 2.5kN. Total fully reversed controlled strains (R_ε=-1 and 0.3%≤ $\Delta\varepsilon_t \leq$0.7%), at a strain rate of $10^{-2}s^{-1}$ were employed. An anti-buckling system, made of aluminium and Teflon®, was employed to prevent specimen buckling during compression phase.

2.3. Metallurgical investigations

Transmission electron micoroscopy (TEM)

TEM samples were taken from post-mortem fatigued specimens. The samples consisted in 3 mm diameter discs with a thickness of 110 µm, twin-jet polished using a solution of 95% acetic acid and 5% perchloric acid at 32V and 20°C. The observations were made on a FEI Technai G2 20 TEM under bright-field imaging (BFI) mode.

Electron backscattered diffraction (EBSD)

SEM-EBSD observations were made on a longitudinal section of an uncracked portion of the lab specimens at mid-plane. After a mechanical polishing down to 0.25µm with diamond paste, followed by a final polishing using 0.02µm colloidal silica solution, the samples were observed in a FEI Quanta 400 SEM fitted with a HKL / Oxford Instruments EBSD system. Post processing analysis was made using Oxford Instruments Channel 5 and TSL OIM 6 commercial softwares.

The Kernel Average Misorientation *(*KAM) approach has been chosen for the quantitative evaluation of the small local strain gradients. As described in literature [2-4], KAM characterises misorientations referring to local orientation gradients. This parameter is calculated by determining the average of all misorientation angles between a point and all its neighbours. The local change in the crystal orientation was evaluated using the local misorientation M_L; its value at point p_0 is calculated by the following equation (1):

$$M_L = \frac{1}{N}\sum_{i=1}^{N}\Delta\theta(P_0, P_i), \quad \Delta\theta \le 5° \tag{1}$$

where $\Delta\theta(P_o, P_i)$ denotes the misorientation between the point p_o and neighbouring points p_i in the same grain as shown in Fig. 2.

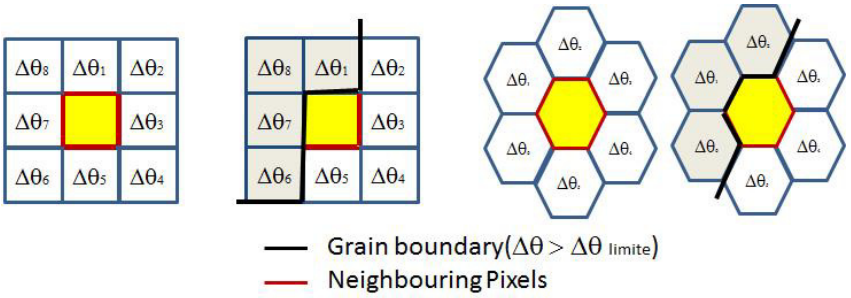

Fig. 2. Definition of local misorientation for square and hexagonal grids

From the EBSD data, the subgrain boundaries have been investigated by means of Low Angle Grain Boundaries ($\Delta\theta<15°$). This marker is generally considered for the description of dislocations structures since those latters exhibit typical misorientation between 2 and 10° [5].

3. Results and discussion

3.1. Cyclic stress response

The evolution of the stress amplitude $\Delta\sigma/2$ versus the number of cycles N in a logarithmic scale and versus the fatigue life fraction in a linear scale are reported in Fig. 3. The fatigue response can be divided into two groups. The first one concerns the tests where the strain range is higher than $\Delta\varepsilon t=0.5\%$. The stress response to strain cycling started first by a short primary hardening rapidly followed by a cyclic softening, and then a secondary hardening occurred before final failure. The transition cycle between the softening phase and the secondary hardening period

decreases with the applied strain amplitude. In the second behaviour type ($\Delta\varepsilon_t$=0.3% - 0.4%), the softening/hardening transition did not occur and the major life time consists of a softening until fracture.

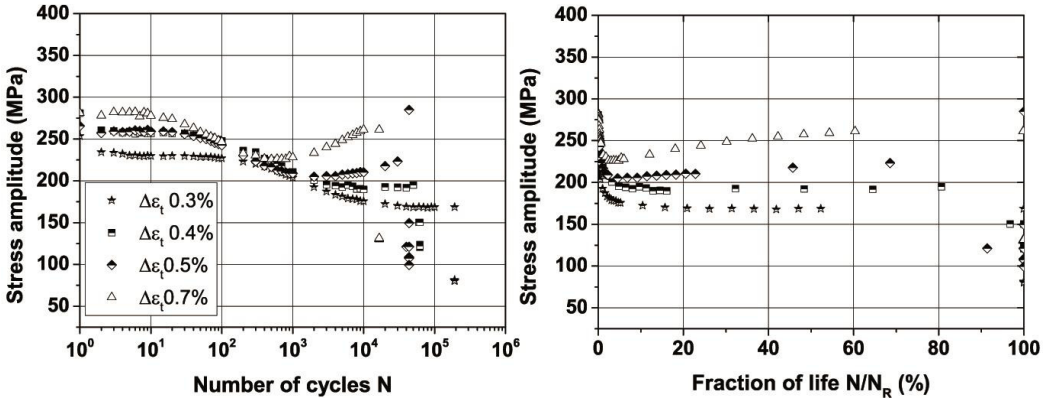

Fig. 3. Cyclic stress response as a function of the number of cycles N (a) and of the life fraction (b) for various strain range tests $\Delta\varepsilon_t$

3.2. Fatigue damage characterization

TEM observations

The TEM micrographs of the unfatigued specimen as well as fatigued samples ($\Delta\varepsilon_t$=0.3%, 0.5% and 0.7%) are shown in Fig. 4. Unfatigued specimen grains appeared to be not totally free of dislocations. Indeed, some grains contained a low but significant amount of entangled dislocations. These were homogenously distributed and probably resulted from the forming process. Cycling the specimen at low strain range ($\Delta\varepsilon_t$=0.3%) resulted in a decrease of dislocations density in comparison with the unfatigued specimen. At low strain amplitude, this slight recovery observed is in agreement with the continuous softening of the material. At the opposite, after fatigue at higher amplitudes, $\Delta\varepsilon$t=0.5% or 0.7%, the specimens contained a high density of dislocations arranged in cells, as often reported for low carbon ferritic steels [1,6]. For the test performed at $\Delta\varepsilon$t=0.7%, the cell size was much smaller than in the case of $\Delta\varepsilon$t=0.5% test. The fatigue dislocations cells related to fatigue are known to be misorientated up to 10° [1,5] and this is evidenced by the contrat between them. Within the cells, the density of dislocations was also high in both cases.

SEM-EBSD observations: Low Angle Grain Boundaries (LAGB)

The LAGB mapping issued from the SEM-EBSD investigations follow the same trend than the TEM observations. Fig. 5 shows the evolution of the LAGB for the fatigued sample at $\Delta\varepsilon$t=0.5%, based on interrupted tests. Here, the LAGB density increases with the applied strain and dislocations cells structure can also be identified. Those observations indicate that the LAGB index is quite sensitive to the accumulated fatigue strain and presents the advantage of being a nondestructive analysis by contrast with the TEM observations since the same sample can be studied for the whole range of its fatigue life.

SEM-EBSD observations: Kernel Average Misorientation (KAM)

The KAM maps corresponding to the unfatigued specimen and the deformed samples ($\Delta\varepsilon$t=0.4% to 0.7%) are reported in Fig. 6. A slight recovery has been observed at $\Delta\varepsilon$t=0.3%. Whereas, $\Delta\varepsilon$t=0.5% and 0.7% specimens, due to large plastic strain, show a high amount of local misorientations. The cumulated plastic strain in the specimen cycled at $\Delta\varepsilon$t=0.7% is so high that local misorientation spreads out in all grains. For the $\Delta\varepsilon$t=0.5% specimen, a lower

strain loading associated to microstructural inhomogeneities lead to the development of a local misorientation in selected grains.

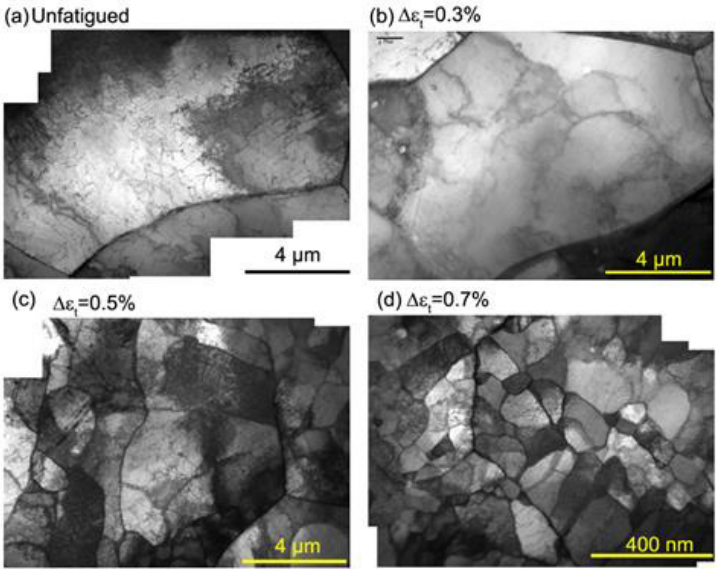

Fig. 4. TEM micrographs of the unfatigued specimen (a), Δεt=0.3% (b), Δεt=0.5% (c) and Δεt=0.7% fatigued specimen (d).

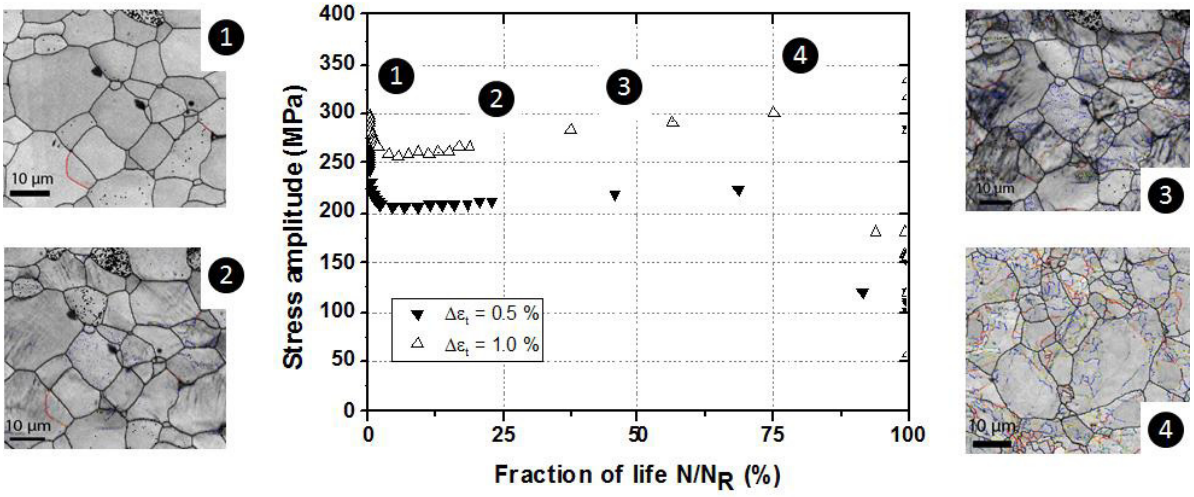

Fig. 5. Evolution of the LAGB mapping for the $\Delta\varepsilon_t$ = 0.5% fatigue sample

In complement, the mean value of this parameter <KAM> has been calculated for each map. By comparing the <KAM> variation of the fatigued samples within the unfatigued specimen (called ΔKAM), a linear relation can be established between ΔKAM and the macroscopic strain (Fig. 7a). It can also be seen on this figure that the evolution of the cell size is not monotonic as can be observed for other metals [7].

Hence, through the mapping of the local deformation as well as the correlation between the macroscopic strain and mean KAM value, the KAM approach confirms its ability to be used as quantitative criteria for fatigue damage assessment.

The SEM-EBSD analysis has been applied in the same way on an ex-service fan. As well, an unused fan is characterized as reference material. Figure 7b reports the measurements of ΔKAM in unused and damaged fans which are then compared to ΔKAM values acquired on lab fatigue specimens.

For the damaged fan, two zones were investigated, one being far from the slot and another one being at the slot root. The first one, though supposed to be undamaged did not exhibit a ΔKAM value equal to zero (ΔKAM= -50) because the forming process induced a slight plastic monotonic deformation. After fatigue, the ΔKAM value calculated from data collected at the slot root reached a value of +50. By comparison with the relation between ΔKAM and plastic strain range obtained from lab experiments, it can be concluded that some slots of fan root the fan were cyclically deformed and the equivalent plastic strain range was about 0.3%.

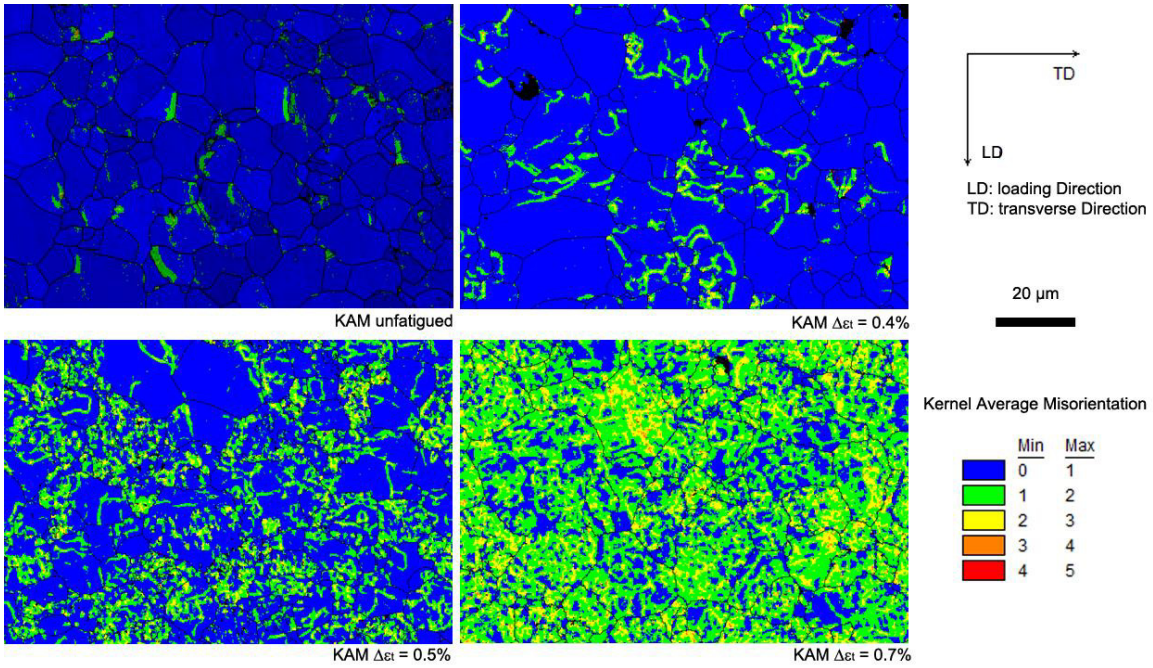

Fig. 6. Color coded SEM-EBSD KAM mapping at different total strain ranges

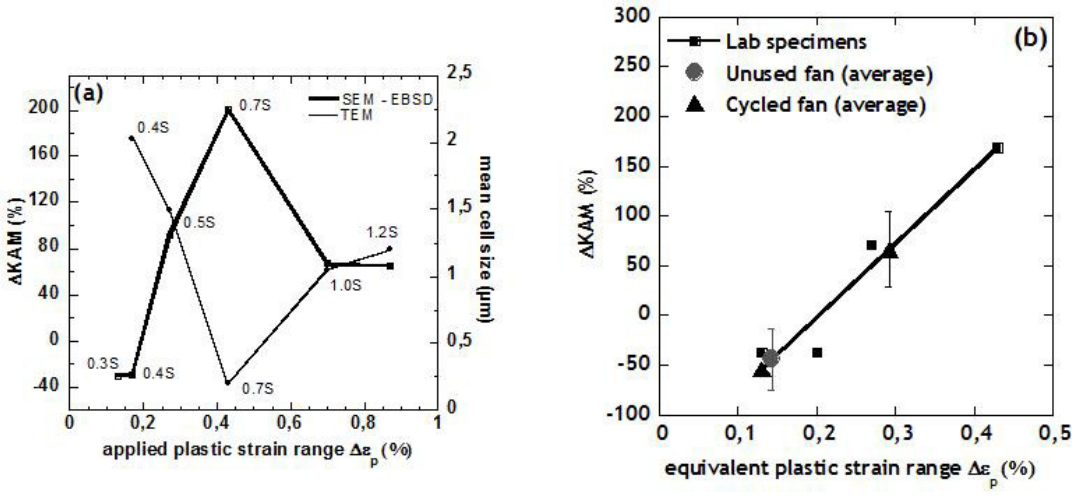

Fig. 7. Variation of ΔKAM and evolution of mean cell size as a function of the plastic strain range obtained on lab specimens (a), and (b) comparison of ΔKAM between lab specimens and fans to deduce the plastic strain range

4. Conclusion

The fatigue behaviour of a ferritic steel has been studied and shows a dependence upon the applied strain range. For the highest strain tests where the cell structure formed, the TEM observations do not allow to easily distinguish the different strain amplitudes except by the cells size. This has been overcome through SEM-EBSD experiments. Dislocation structures were imaged and associated with LAGB identifications, and the local strain evolution evaluated with the KAM approach method. The method has been applied to a component fatigued in service. An equivalent plastic strain range of about 0.3% has been determined.

Acknowledgements

This work was supported by the French Environment and Energy Management Agency (ADEME) and Valeo Engine Electrical Systems. The authors thank J. Golek and D. Creton for their technical assistance.

References

[1] J.-B. Vogt, S. Argillier,J.-P. Massoud, V. Prunier, Eng. Fail. Ana. 7, 2000, 301-310
[2] M. Kamaya, Materials characterization, 66, 2012, 56 – 67
[3] Allain-Bonasso, N. Wagner, F. Berbenni, S. Field, D. P, Mater. Sci. Eng. A, 2012,.56-63.
[4] S.-I. Wright, M.-M. Nowell, D.-P. Field, Microsc. Microanal. 17, 2011, 316-329
[5] A. Godfrey, W.Q. Cao, N. Hansen, Q. Liu, Metal. Mater. Trans. 36A, 2005, 2371-2378
[6] C-C Shih, N-J Ho, H-L Huang, Materials characterization, 60, 2009, 1280-1288
[7] E.S. Kayali, A. Plumtree, Metal. Trans. 13A, 1982, 1033-1041